



Modern Method for the Preparation of Some Metal Oxides in the Form of Nanometric Feature using Schiff Base Complexes as Precursors: Synthesis, Characterization and Antibacterial Properties

F. A. KORA^{1,3*}, A. I. EL-SHAWY^{1,4} and M.S. REFAT^{2,5}

¹Department of Chemistry, Collage of Education, Dammam University, Kingdom of Saudi Arabia.

²Department of Chemistry, Faculty of Science, Taif University, 888 Taif, Kingdom of Saudi Arabia.

³Department of Chemistry, Faculty of Science, Alazhar University, Nasr-City, Cairo, Egypt.

⁴Department of Chemistry, Faculty of Science, Benha University, Benha, Egypt.

⁵Department of Chemistry, Faculty of Science, Port Said, Port Said University, Egypt.

*Corresponding author E-mail: fkourah_51@hotmail.com

(Received: January 26, 2013; Accepted: March 16, 2013)

ABSTRACT

Metal complexes, ML_2X_2 , where M is Mn(II), Co(II) or Cu(II), X = (NO₃⁻ or Cl⁻), and L is the Schiff base formed by condensation of 2-thiophenecarboxaldehyde with phenyl hydrazine have been prepared and characterized by elemental analysis, magnetic and spectroscopic measurements (infrared, Raman, X-ray powder diffraction and scanning electron microscopy). Elemental analysis of the chelates suggests the stoichiometry is 1:2 (metal-ligand). Infrared spectra of the complexes agree with the coordination to the central metal atom through the nitrogen of the phenyl hydrazine (-Ph-NH-) group and the sulfur atom of the thiophene ring. Magnetic susceptibility data coupled with electronic spectra suggest a distorted octahedral structure for all Schiff base complexes. The Schiff base and its metal chelates have been screened for their in vitro antibacterial activity against four bacteria, gram-positive (*Bacillus subtilis* and *Staphylococcus aureus*) and gram-negative (*Escherichia coli* and *Pseudomonas aeruginosa*) and two strains of fungus (*Aspergillus flavus* and *Candida albicans*). The metal chelates were shown to possess more antibacterial activity than the free Schiff-base chelate.

Key words: Spectroscopic, Transition metal complexes, Schiff base, Thermal analysis.

INTRODUCTION

The synthesis of metal oxide nanoparticle has received considerable attention with their potential applications in various fields. Nanotechnology offers unique approaches to probe and control a variety of biological and medical processes that occur at nanometer length scales,

and is expected to have a revolutionary impact on biology and medicine. Among the approaches for exploiting nanotechnology in medicine, nanoparticles offer some unique advantages as sensing, image enhancement, and delivery agents. Several varieties of nanoparticles with biomedical relevance are available including, polymeric nanoparticles, metal nanoparticles, liposomes,

micelles, quantum dots, dendrimers, and nano-assemblies. To further the application of nanoparticles in disease diagnosis and therapy, it is important that the systems are biocompatible and capable of being functionalized for recognition of specific target sites in the body after systemic administration.

Schiff base ligands are considered "privileged ligands" because they are easily prepared by the condensation between aldehydes and imines. Stereogenic centers or other elements of chirality (planes, axes) can be introduced in the synthetic design. Schiff base ligands are able to coordinate with many different metals¹, and to stabilize them in various oxidation states. The Schiff base complexes have been used in catalytic reactions² and as models for biological systems³. Chiral Schiff bases derived from the condensation of salicylaldehydes with 2-amino alcohols have found widespread use as ligands in asymmetric synthesis. These compounds act as tridentate ONO ligands, and a great number of metallic complexes derived from them have been described in the literature⁴. Depending upon the nature of the metal centre, these chiral complexes are able to promote a variety of enantioselective transformations. It has been reported that the structure of the substituent bonded to the imino nitrogen affects the coordination geometry of the complex⁵. During the past two decades, considerable attention has been paid to the chemistry of the metal complexes of Schiff bases containing nitrogen and other donors⁶. This may be attributed to their stability, biological activity⁷ and potential applications in many fields such as oxidation catalysis, electrochemistry⁸. The complexes make these compounds effective and stereospecific catalysts for oxidation, reduction and hydrolysis and they show biological activity, and other transformations of organic and inorganic chemistry. It is well known that some drugs have higher activity when administered as metal complexes than as free ligands⁹.

Nickel(II) complexes containing sulfur donors have received considerable attention due to the identification of a sulfur rich coordination environment in biological nickel centers, such as the active sites of certain ureases, methyl-S-coenzyme-M-methyl reductase and

hydrogenases¹⁰. The zinc(II) ion is known to have a high affinity towards nitrogen and sulfur donor ligands. Dowling and Perkin investigated Zn(II) complexes with mixed N, O and S coordination to understand the reactivity of the pseudo-tetrahedral zinc center in proteins¹¹. The transition metals zinc and copper are some of the most frequently occurring elements integrated into essential biochemical pathways. There are a number of biologically important molecules showing the catalytic activity¹² or molecules involved in transfer processes, like oxygen transfer, and incorporating transition metals into their active sites. In contrast to zinc(II), the copper(II) ions are redox active and play a crucial role in catalytic sites of oxidoreductases. The cyclic redox process enables these ions to act as pro- or anti-oxidants. The published opinions on the structure and pro- or anti-oxidant activity relationships are, however, quite inconsistent¹³. We report herein the results of our studies on the metal complexes of a Schiff base derived from 2-thiophenecarboxaldehyde and phenylhydrazine. Tentative structures have been proposed on the basis of analytical, spectral, magnetic, and conductance data. In order to establish a modern technique to prepare some of nanometric oxide using Schiff base compounds and collected the biological role of metals, this prepared Schiff base and its metal chelates have been screened for biological activity against some kind of bacterial (G⁺ and G⁻) and fungi.

EXPERIMENTAL

Chemicals

Reagent grade 2-thiophenecarboxaldehyde, phenyl hydrazine, and transition metal salts (manganese(II) chloride tetrahydrate, cobalt(II) nitrate hexahydrate, and copper(II) chloride dihydrate) were received from BDH and Aldrich Companies, and other chemicals and solvents were purchased and used as received. 2-2- Synthesis of the bi-dentate Schiff base (PTMH) The Schiff base (PTMH, Fig. 1) was been prepared according to the previous procedure^{14,15}: An ethanolic solution of 2-thiophenecarboxaldehyde (1 mmol, 25 mL) was added to an ethanolic solution of phenyl hydrazine (1 mmol, 25 mL) and refluxed for 2 hour in a water bath. After concentration of the solution, the precipitate was separated, filtered,

washed with ethanol, and dried over anhydrous calcium chloride under vacuum. Anal.: Calcd. for PTMH: C, 65.32; H, 4.98; N, 13.85; S, 15.85. Found: C, 65.12; H, 4.78; N, 13.74; S, 15.59. The calculated mass spectrum: m/e: 202.056 (100.0%), 203.060 (12.2%), 204.052 (4.4%).

Synthesis of the ML_2X_2 Schiff base complexes

A mixture of PTMH (2 mmol, 50 mL) in ethanol was added to an ethanolic solution of manganese(II) chloride tetrahydrate, cobalt(II) nitrate hexahydrate, or copper(II) chloride dihydrate (1 mmol, 50 mL). The mixture of reaction was refluxed for 2 hours and then excess solvent was distilled. The precipitated compounds that separated were filtered, washed with ethanol, and dried over $CaCl_2$ in vacuum. Anal.: Calcd. for MnL_2Cl_2 : C, 49.82; H, 3.80; N, 10.56; S, 12.09. Found: C, 49.11; H, 3.53; N, 10.09; S, 11.93. Anal.: Calcd. for $CoL_2(NO_3)_2$: C, 44.98; H, 3.43; N, 14.30; S, 10.92. Found: C, 44.76; H, 3.31; N, 14.21; S, 10.83. Anal.: Calcd. for CuL_2Cl_2 : C, 49.02; H, 3.74; N, 10.39; S, 11.90. Found: C, 48.56; H, 3.60; N, 10.22; S, 11.52.

Measurements

The elemental analyses of carbon, hydrogen, nitrogen and sulfur contents were performed using a Perkin Elmer CHNS 2400 (USA). The molar conductivities of freshly prepared 1.0×10^{-3} mol/cm³ dimethylsulfoxide (DMSO) solutions were measured for the dissolved PTMH Schiff base Mn(II), Co(II) and Cu(II) complexes using Jenway 4010 conductivity meter. The electronic absorption spectra of PTMH Schiff base complexes were recorded in DMSO solvent within 900-200 nm range using a UV2 Unicam UV/Vis Spectrophotometer fitted with a quartz cell of 1.0 cm path length. The infrared spectra with KBr discs were recorded on a Bruker FT-IR Spectrophotometer ($4000-400$ cm⁻¹), while Raman laser spectra of samples were measured on the Bruker FT-Raman with laser 50 mW. Magnetic data were calculated using Magnetic Susceptibility Balance, Sherwood Scientific, Cambridge Science Park Cambridge, England, at Temp 25°C. The thermal studies TG/DTG-50H were carried out on a Shimadzu thermogravimetric analyzer under static air till 300 °C. Scanning electron microscopy (SEM) images were taken in Quanta FEG 250 equipment. The X-ray diffraction patterns for the Mn^{II}, Co^{II} and Cu^{II} Schiff base

complexes were recorded on X 'Pert PRO PAN-analytical X-ray powder diffraction, target copper with secondary monochromate.

Antibacterial and antifungal evaluation

Antimicrobial activity of the tested samples was determined using a modified Kirby-Bauer disc diffusion method¹⁶. Briefly, 100 µl of the tested bacteria/fungi were grown in 10 mL of fresh media until they reached a count of approximately 10⁸ cells/mL for bacteria or 10⁵ cells/mL for fungi¹⁷. 100 µl of microbial suspension was spread onto agar plates corresponding to the broth in which they were maintained. Isolated colonies of each organism that might be playing a pathogenic role should be selected from primary agar plates and tested for susceptibility by disc diffusion method^{18, 19}.

Of the many media available, National Committee for Clinical Laboratory Standards (NCCLS) recommends Mueller-Hinton agar due to: it results in good batch-to-batch reproducibility. Disc diffusion method for filamentous fungi tested by using approved standard method (M38-A) developed by the NCCLS²⁰ for evaluating the susceptibility of filamentous fungi to antifungal agents. Disc diffusion method for yeast developed standard method (M44-P) by the NCCLS²¹. Plates inoculated with filamentous fungi as *Aspergillus Flavus* at 25 °C for 48 hours; Gram (+) bacteria as *Staphylococcus Aureus*, *Bacillus subtilis*; Gram (-) bacteria as *Escherichia Coli*, *Pseudomonas aeruginosa* they were incubated at 35-37 °C for 24-48 hours and yeast as *Candida Albicans* incubated at 30 °C for 24-48 hours and, then the diameters of the inhibition zones were measured in millimeters¹⁶. Standard discs of Tetracycline (Antibacterial agent), Amphotericin B (Antifungal agent) served as positive controls for antimicrobial activity but filter disc impregnated with 10 µl of solvent (distilled water and DMSO) were used as a negative control.

The agar used is Mueller-Hinton agar that is rigorously tested for composition and pH. Further the depth of the agar in the plate is a factor to be considered in the disc diffusion method. This method is well documented and standard zones of inhibition have been determined for susceptible

values. Blank paper disks (Schleicher & Schuell, Spain) with a diameter of 8.0 mm were impregnated 10 μ l of tested concentration of the stock solutions. When a filter paper disc impregnated with a tested chemical is placed on agar the chemical will diffuse from the disc into the agar. This diffusion will place the chemical in the agar only around the disc. The solubility of the chemical and its molecular size will determine the size of the area of chemical infiltration around the disc. If an organism is placed on the agar it will not grow in the area around the disc if it is susceptible to the chemical. This area of no growth around the disc is known as a "Zone of inhibition" or "Clear zone". For the disc diffusion, the zone diameters were measured with slipping calipers of the National for Clinical Laboratory Standards¹⁸. Agar-based methods such as disk diffusion test can be good alternatives because they are simpler and faster than broth methods^{22, 23}.

RESULTS AND DISCUSSIONS

The synthesized complexes of Mn(II), Co(II) and Cu(II) with the Schiff base PTMH (Fig. 1) appeared as powders with high melting points (Table 1). They are not soluble in ethanol, diethyl ester, or chloroform, but are soluble in DMSO and DMF. Elemental analysis suggests that the complexes have 1:2 (metal-ligand) stoichiometry. The molar conductance of the Mn(II), Co(II) and Cu(II) Schiff

base complexes in DMSO are low, indicating there are non-electrolytic nature. Based on the elementary chemical analysis the formula, ML_2X_2 , was suggested for all compounds.

Some characteristic infrared absorption bands of PTMH and its Mn^{II}, Co^{II} and Cu^{II} complexes, along with their assignments, are presented in Table 2. The infrared spectrum of the ligand (Fig. 2) exhibits a band at 1599 cm^{-1} assignable to $\nu(\text{C}=\text{N})$ of the azomethine group and an intense bands at (1536, 1507 and 1447) cm^{-1} corresponding to the C=C stretching of the benzene and thiophene rings. The comparison of the positions of these bands with those observed in the IR spectra of the manganese(II), cobalt(II) and copper(II) complexes indicated that the band at 1599 cm^{-1} did not show a marked shift, this discussed that azomethine group unshared in the complexation toward Mn(II), Co(II) and Cu(II) ions, while that band at 3322 cm^{-1} which assigned to $-\text{NH}$ of phenylhydrazine moiety is a mild decreasing in an intensity and shifted to a slightly lower region by about $\sim 5 \text{ cm}^{-1}$. This behavior suggests the coordination of PTMH through the Ph-NH nitrogen of phenylhydrazine. Proof of coordination to the N atom is provided by the occurrence of the new bands at $\sim 420 \text{ cm}^{-1}$ in the IR spectra of the complexes. The observed medium intensity band at 910 cm^{-1} in the free ligand, which is ascribed to $\nu(\text{CSC})$ of thiophene ring stretching

Table 1: Analytical and physical data for PTMH Schiff base complexes

Compounds	Mp ($^{\circ}\text{C}$)	Color	L_m ($\text{W}^{-1}\text{cm}^2\text{mol}^{-1}$)
$[\text{Mn}(\text{PTMH})_2\text{Cl}_2]$	235	Light brown	35
$[\text{Co}(\text{PTMH})_2(\text{NO}_3)_2]$	224	Dark brown	28
$[\text{Cu}(\text{PTMH})_2\text{Cl}_2]$	237	Light brown	32

Table 2: Infrared characteristic bands frequencies (cm^{-1}) of the ligand complexes

Compounds	$\nu(\text{C}=\text{N})$	$\nu(\text{C}=\text{C})$ phenyl + thiophene	$\nu(\text{CSC})$	$\nu_{\text{as}}(\text{C}-\text{S})$	$\nu(\text{M}-\text{N})$
PTMH	1599	1536, 1507, 1447	910	705	-
$[\text{Mn}(\text{PTMH})_2\text{Cl}_2]$	1599	1535, 1504, 1451	884	688	421
$[\text{Co}(\text{PTMH})_2(\text{NO}_3)_2]$	1599	1542, 1496, 1451	884	695	415
$[\text{Cu}(\text{PTMH})_2\text{Cl}_2]$	1599	1535, 1503, 1445	884	688	421

Table 3: Antimicrobial activity data of PTMH and its Mn(II), Co(II) and Cu(II) complexes

Sample	Inhibition zone diameter (mm / mg sample)						
	<i>Bacillus subtilis</i> (G ⁺)	<i>Escherichia coli</i> (G ⁻)	<i>Pseudomonas aeruginosa</i> (G ⁻)	<i>Staphylococcus aureus</i> (G ⁺)	<i>Aspergillus flavus</i> (Fungus) <i>albicans</i> (Fungus)	<i>Candida</i>	
Control: DMSO	0.0	0.0	0.0	0.0	0.0	0.0	0.0
Antibacterial agent	34	32	34	30	—	—	—
Amphotericin B	—	—	—	—	18	19	19
Antifungal agent	9.0	8.0	12	11	5.0	3.0	3.0
PTMH	7.0	11	8.0	11	0.0	4.0	4.0
Mn(II)	10	6.0	4.0	9.0	6.0	2.0	2.0
Co(II)	12	14	10	17	0.0	6.0	6.0
Cu(II)							

vibration¹⁵, shifted to lower values for the three complexes, suggesting the involvement of the sulfur atom in the bonding with the metal's ions. The band assigned to the asymmetric $\nu(\text{C-S})$ is similarly shifted. This also confirms that the sulfur atom is taking part in the complex formation¹⁵.

On the other hand, the spectra of PTMH, $[\text{Co}(\text{PTMH})_2(\text{NO}_3)_2]$ and $[\text{Cu}(\text{PTMH})_2\text{Cl}_2]$ Schiff base complex (Fig. 3) has a sharp broadening with distorted in the stretching vibration bands, this can be discussed under the knowledge that Raman analysis of fluorescent materials and compounds is a challenging task experimentally due to the overlap of fluorescence which, even when very weak, can overwhelm the inherently weak Raman scattering signal²⁵⁻²⁷.

It is tentatively suggested that the Schiff base ligand coordinates through the nitrogen of the phenyl hydrazine moiety and the sulfur of the thiophene ring, forming a stable chelating structure. According to the above discussion, distorted octahedral structures for Mn(II), Co(II) and Cu(II) complexes are drawn in Fig. 4.

Upon the electronic spectrum of the N-Phenyl-N'-thiophen-2-ylmethylene-hydrazine (PTMH) Schiff base ligand, the two essential absorption bands were observed at 266 nm, (361 and 436) nm and assigned to the transitions $n \rightarrow \pi^*$, $\pi \rightarrow \pi^*$, respectively. These transitions were existed also in the spectra of the complexes, but they shifted to lower intensities, confirming the coordination of the ligand to the metal ions. Information concerning the geometry of these compounds was obtained from the electronic spectra and from magnetic moment values. The electronic spectrum of the Mn(II) complex shows four medium intensity bands assigned to ${}^6\text{A}_{1g} \rightarrow {}^4\text{T}_{1g}(\text{G})$, ${}^6\text{A}_{1g} \rightarrow {}^4\text{T}_{2g}(\text{G})$, and ${}^6\text{A}_{1g} \rightarrow {}^4\text{E}_g(\text{G})$, ${}^4\text{A}_{1g}(\text{G})$, respectively, for an Mn(II) ion in an distorted octahedral field [26]. The electronic spectrum of octahedral Co^{II} complex has three types of transitions due to ${}^4\text{T}_{1g}(\text{F}) \rightarrow {}^4\text{A}_{2g}(\text{F})$, and ${}^4\text{T}_{1g}(\text{F}) \rightarrow {}^4\text{T}_{2g}(\text{P})$ [26]. The diffuse reflectance spectrum of copper(II) complex is expected to show two allowed transitions namely ${}^2\text{B}_{1g} \rightarrow {}^2\text{E}_g$ and ${}^2\text{B}_{1g} \rightarrow {}^2\text{B}_{2g}$. These bands suggested distorted octahedral geometry around Cu(II)²⁷.

Magnetic susceptibility measurement in a magnetic field, the paramagnetic complexes will be attracted while the diamagnetic compounds repelled. In paramagnetic Mn(II), Co(II) and Cu(II) complexes, often the magnetic moment (μ_{eff}) gives the spin only value ($\mu_{\text{s.o.}} = (n(n+2))^{1/2}$ B.M.) corresponding to the number of unpaired electron. The variation from the spin only value is attributed to the orbital contribution and it varies with the nature of coordination and consequent delocalization. The octahedral geometry of Co(II) complex has a magnetic moments, number of unpaired electrons, corresponding to configuration and expected value as 5.50 BM, 4, d^6 and 5.39. These complexes have an experimental values are higher than expected values; this can be discussed on the fact that the presence of magnetic centers coupled together²⁶. The magnetic moment, configurations, stereochemistry, hybrid orbitals, number of unpaired electrons and expected magnetic values of copper(II) and manganese(II) Schiff base complexes are (1.84 B.M., d^9 , octahedral, sp^3d^2 , 1, 1.96 B.M.) and (5.54 B.M., d^5 , octahedral, sp^3d^2 , 5, 6.00 B.M.), respectively. The lower magnetic value of Cu(II) and Mn(II) of PTMH complexes assigned to that individual magnetic moments are aligned in opposite directions so that they cancel each other to some extent or can be ascribed as due antiferromagnetic coupling. Thus the value of magnetic moment of a complex would give valuable insights into its constitution and structure. The magnetic susceptibility measurements thus help to predict the possible geometry of the metal complexes.

The manganese(II), cobalt(II) and copper(II) oxides nanoparticles were synthesized at 600 °C using $[\text{Mn}(\text{PTMH})_2\text{Cl}_2]$, $[\text{Co}(\text{PTMH})_2(\text{NO}_3)_2]$ and $[\text{Mn}(\text{PTMH})_2\text{Cl}_2]$ Schiff base complexes as precursors and their properties studied with the help of a scanning electron microscope (SEM) and X-ray diffraction. Figs. 5, 6 shows the SEM image of the synthesized MnO, CoO and CuO nano-particles, with an image magnification. The assembly was attached to a computer running a program to analyze the mean size of the particles in the samples. It should be noted that the particle diameter is always overestimated due to the distortion of SEM images²⁷.

Figure 6a-c demonstrates the XRD patterns of the synthesized MnO, CoO and CuO nanoparticles. The X-ray diffraction data were recorded by using Cu K α radiation (1.5406 Angstrom). The intensity data were collected over a 2θ range of 4–80°. The average grain size of the samples was estimated with the help of the Scherrer equation, using the diffraction intensity peak. X-ray diffraction studies confirmed that the synthesized materials were MnO, CoO and CuO and all the diffraction peaks agreed with the reported standard data; no characteristic peaks were observed other than oxide, MO. The mean grain size (D) of the particles was determined from the XRD line broadening measurement using the Scherrer Equation (1):

$$D = 0.89\lambda/(\beta\cos\theta) \quad \dots(1)$$

Where λ is the wavelength (Cu K α), β is the full width at the half- maximum (FWHM) of the MnO, CoO and CuO line and θ is the diffraction angle. A definite line broadening of the diffraction peaks is an indication that the synthesized materials are in the nanometer range. The lattice parameters calculated were also in agreement with the reported values. The reaction temperature greatly influences the particle morphology of as-prepared MnO, CoO and CuO powders.

The results of nanoparticle size measurement of samples by XRD and SEM indicate

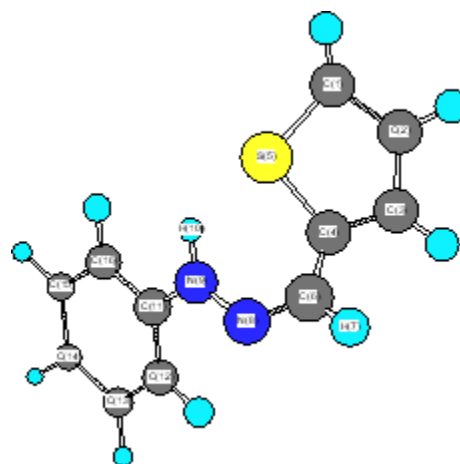


Fig. 1: Structure of Schiff base N-Phenyl-N'-thiophen-2-ylmethylene-hydrazine (PTMH)

Table 4: The values of bond lengths and bond angles of PTMH Schiff base and its manganese(II) complex

Adducts	Bond length (Atoms_Actual_Optimal)		Bond angle (Atoms_Actual_Optimal)			
Ligand	C(1)-C(2)	1.550	1.337	C(2)-C(1)-S(5)	97.155	119.000
	C(1)-S(5)	1.856	1.856	C(2)-C(1)-H(22)	131.423	120.000
	C(1)-H(22)	1.100	1.100	S(5)-C(1)-H(22)	131.416	120.000
	C(2)-C(3)	1.503	1.503	C(1)-C(2)-C(3)	122.346	120.000
	C(2)-H(23)	1.100	1.100	C(1)-C(2)-H(23)	118.826	120.000
	C(3)-C(4)	1.337	1.337	C(3)-C(2)-H(23)	118.825	120.000
	C(3)-H(24)	1.100	1.100	C(2)-C(3)-C(4)	110.998	120.000
	C(4)-S(5)	1.856	1.856	C(2)-C(3)-H(24)	124.499	120.000
	C(4)-C(6)	1.503	1.503	C(4)-C(3)-H(24)	124.497	120.000
	C(6)-N(8)	1.260	1.260	C(3)-C(4)-S(5)	111.000	119.000
	C(6)-H(7)	1.100	1.100	C(3)-C(4)-C(6)	120.001	120.000
	N(8)-N(9)	1.426	1.426	S(5)-C(4)-C(6)	119.000	119.000
	N(9)-C(11)	1.462	1.462	C(1)-S(5)-C(4)	98.500	98.500
	N(9)-H(10)	1.050	1.050	C(4)-C(6)-N(8)	123.499	123.500
	C(11)-C(12)	1.420	1.420	C(4)-C(6)-H(7)	119.998	120.000
	C(11)-C(16)	1.420	1.420	H(7)-C(6)-N(8)	116.503	116.500
	C(12)-C(13)	1.420	1.420	C(6)-N(8)-N(9)	115.001	115.000
	C(12)-H(21)	1.100	1.100	N(8)-N(9)-C(11)	125.668	124.000
	C(13)-C(14)	1.420	1.420	N(8)-N(9)-H(10)	114.668	113.000
	C(13)-H(19)	1.100	1.100	H(10)-N(9)-C(11)	119.662	118.000
	C(14)-C(15)	1.420	1.420	N(9)-C(11)-C(12)	119.998	120.000
	C(14)-H(18)	1.100	1.100	N(9)-C(11)-C(16)	119.998	120.000
	C(15)-C(16)	1.420	1.420	C(12)-C(11)-C(16)	120.001	120.000
	C(15)-H(17)	1.100	1.100	C(11)-C(12)-C(13)	119.998	120.000
	C(16)-H(20)	1.100	1.100	C(11)-C(12)-H(21)	120.001	120.000
				C(13)-C(12)-H(21)	119.998	120.000
				C(12)-C(13)-C(14)	120.000	120.000
				C(12)-C(13)-H(19)	119.998	120.000
				C(14)-C(13)-H(19)	119.998	120.000
				C(13)-C(14)-C(15)	120.000	120.000
				C(13)-C(14)-H(18)	119.998	120.000
				C(15)-C(14)-H(18)	120.000	120.000
			C(14)-C(15)-C(16)	120.001	120.000	
			C(14)-C(15)-H(17)	119.998	120.000	
			C(16)-C(15)-H(17)	119.998	120.000	
			C(11)-C(16)-C(15)	119.998	120.000	
			C(11)-C(16)-H(20)	119.998	120.000	
			C(15)-C(16)-H(20)	120.003	120.000	
Mn ²⁺	C(1)-C(2)	1.829	1.337	C(2)-C(1)-Mn(5)	87.320	
	C(1)-Mn(5)	1.940		C(2)-C(1)-H(50)	150.017	120.000
	C(1)-H(50)	1.100	1.100	Mn(5)-C(1)-H(50)	122.659	
	C(2)-C(3)	1.503	1.503	C(1)-C(2)-C(3)	126.062	120.000
	C(2)-H(51)	1.100	1.100	C(1)-C(2)-H(51)	132.358	120.000
	C(3)-C(4)	1.337	1.337	C(3)-C(2)-H(51)	101.577	120.000
	C(3)-H(52)	1.100	1.100	C(2)-C(3)-C(4)	111.000	120.000
	C(4)-Mn(5)	1.940		C(2)-C(3)-H(52)	124.497	120.000
	C(4)-C(6)	1.503	1.503	C(4)-C(3)-H(52)	124.497	120.000
	Mn(5)-Mn(34)	2.340		C(3)-C(4)-Mn(5)	111.000	
	Mn(5)-H(53)	1.522		C(3)-C(4)-C(6)	120.001	120.000
	Mn(5)-H(54)	1.522		Mn(5)-C(4)-C(6)	119.998	
	C(6)-N(8)	1.740	1.260	C(1)-Mn(5)-C(4)	104.501	
	C(6)-H(7)	1.100	1.100	C(1)-Mn(5)-Mn(34)	119.998	
	N(8)-N(9)	1.352		C(1)-Mn(5)-H(53)	180.000	
	N(9)-C(11)	1.446		C(1)-Mn(5)-H(54)	40.893	
	N(9)-Mn(34)	1.846		C(4)-Mn(5)-Mn(34)	120.001	
	N(9)-H(10)	1.028		C(4)-Mn(5)-H(53)	75.501	
	C(11)-C(12)	1.420	1.420	C(4)-Mn(5)-H(54)	120.000	
	C(11)-C(16)	1.420	1.420	Mn(34)-Mn(5)-H(53)	60.001	
C(12)-C(13)	1.420	1.420	Mn(34)-Mn(5)-H(54)	119.998		

Mn ²⁺	C(1)-C(2)	1.829	1.337	C(2)-C(1)-Mn(5)	87.320	
	C(1)-Mn(5)	1.940		C(2)-C(1)-H(50)	150.017	120.000
	C(1)-H(50)	1.100	1.100	Mn(5)-C(1)-H(50)	122.659	
	C(2)-C(3)	1.503	1.503	C(1)-C(2)-C(3)	126.062	120.000
	C(2)-H(51)	1.100	1.100	C(1)-C(2)-H(51)	132.358	120.000
	C(3)-C(4)	1.337	1.337	C(3)-C(2)-H(51)	101.577	120.000
	C(3)-H(52)	1.100	1.100	C(2)-C(3)-C(4)	111.000	120.000
	C(4)-Mn(5)	1.940		C(2)-C(3)-H(52)	124.497	120.000
	C(4)-C(6)	1.503	1.503	C(4)-C(3)-H(52)	124.497	120.000
	Mn(5)-Mn(34)	2.340		C(3)-C(4)-Mn(5)	111.000	
	Mn(5)-H(53)	1.522		C(3)-C(4)-C(6)	120.001	120.000
	Mn(5)-H(54)	1.522		Mn(5)-C(4)-C(6)	119.998	
	C(6)-N(8)	1.740	1.260	C(1)-Mn(5)-C(4)	104.501	
	C(6)-H(7)	1.100	1.100	C(1)-Mn(5)-Mn(34)		119.998
	N(8)-N(9)	1.352		C(1)-Mn(5)-H(53)	180.000	
	N(9)-C(11)	1.446		C(1)-Mn(5)-H(54)	40.893	
	N(9)-Mn(34)	1.846		C(4)-Mn(5)-Mn(34)		120.001
	N(9)-H(10)	1.028		C(4)-Mn(5)-H(53)	75.501	
	C(11)-C(12)	1.420	1.420	C(4)-Mn(5)-H(54)	120.000	
	C(11)-C(16)	1.420	1.420	Mn(34)-Mn(5)-H(53)		60.001
	C(12)-C(13)	1.420	1.420	Mn(34)-Mn(5)-H(54)		119.998
	C(12)-H(48)	1.100	1.100	H(53)-Mn(5)-H(54)		139.108
	C(13)-C(14)	1.420	1.420	C(4)-C(6)-N(8)	101.612	123.500
	C(13)-H(46)	1.100	1.100	C(4)-C(6)-H(7)	134.684	120.000
	C(14)-C(15)	1.420	1.420	H(7)-C(6)-N(8)	123.700	116.500
	C(14)-H(40)	1.100	1.100	C(6)-N(8)-N(9)	135.336	
	C(15)-C(16)	1.420	1.420	N(8)-N(9)-C(11)	109.472	
	C(15)-H(39)	1.100	1.100	N(8)-N(9)-Mn(34)	109.470	
	C(16)-H(47)	1.100	1.100	N(8)-N(9)-H(10)	109.489	
	C(17)-C(18)	1.503	1.503	C(11)-N(9)-Mn(34)		109.470
	C(17)-S(21)	1.554		H(10)-N(9)-C(11)	109.470	
	C(17)-H(49)	1.100	1.100	H(10)-N(9)-Mn(34)		109.456
	C(18)-C(19)	1.591	1.337	N(9)-C(11)-C(12)	120.000	
	C(18)-H(44)	1.100	1.100	N(9)-C(11)-C(16)	120.000	
	C(19)-C(20)	1.503	1.503	C(12)-C(11)-C(16)		119.998 120.000
	C(19)-H(45)	1.100	1.100	C(11)-C(12)-C(13)		120.000 120.000
C(20)-S(21)	1.554		C(11)-C(12)-H(48)		119.998 120.000	
C(20)-C(23)	1.503	1.503	C(13)-C(12)-H(48)		120.000 120.000	
S(21)-Mn(34)	2.190		C(12)-C(13)-C(14)		120.000 120.000	
S(21)-H(22)	1.346	1.346	C(12)-C(13)-H(46)		119.998 120.000	
C(23)-N(25)	1.485	1.260	C(14)-C(13)-H(46)		120.000 120.000	
C(23)-H(24)	1.100	1.100	C(13)-C(14)-C(15)		120.001 120.000	
N(25)-N(26)	1.352		C(13)-C(14)-H(40)		119.998 120.000	
N(26)-C(28)	1.446		C(15)-C(14)-H(40)		119.998 120.000	
N(26)-Mn(34)	1.846		C(14)-C(15)-C(16)		119.998 120.000	
N(26)-H(27)	1.028		C(14)-C(15)-H(39)		120.000 120.000	
C(28)-C(29)	1.420	1.420	C(16)-C(15)-H(39)		119.998 120.000	
C(28)-C(33)	1.420	1.420	C(11)-C(16)-C(15)		120.001 120.000	
C(29)-C(30)	1.420	1.420	C(11)-C(16)-H(47)		119.998 120.000	
C(29)-H(43)	1.100	1.100	C(15)-C(16)-H(47)		119.998 120.000	
C(30)-C(31)	1.420	1.420	C(18)-C(17)-S(21)		110.998	
C(30)-H(41)	1.100	1.100	C(18)-C(17)-H(49)		124.502 120.000	
C(31)-C(32)	1.420	1.420	S(21)-C(17)-H(49)		124.497	
C(31)-H(38)	1.100	1.100	C(17)-C(18)-C(19)		106.749 120.000	
C(32)-C(33)	1.420	1.420	C(17)-C(18)-H(44)		126.620 120.000	
C(32)-H(37)	1.100	1.100	C(19)-C(18)-H(44)		126.627 120.000	
C(33)-H(42)	1.100	1.100	C(18)-C(19)-C(20)		106.751 120.000	
Mn(34)-Cl(35)	2.160		C(18)-C(19)-H(45)		126.623 120.000	
Mn(34)-Cl(36)	2.160		C(20)-C(19)-H(45)		126.623 120.000	
			C(19)-C(20)-S(21)		110.998	
			C(19)-C(20)-C(23)		128.998 120.000	
			S(21)-C(20)-C(23)		119.998	

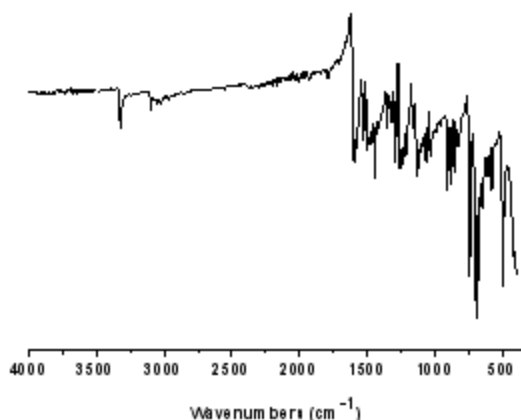


Fig. 2(a): Infrared spectrum of Schiff base PTMH free ligand

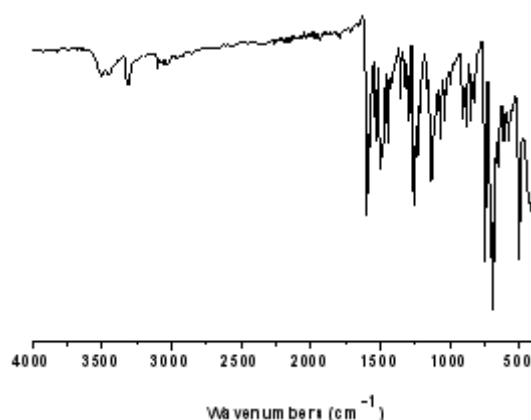


Fig. 2(b): Infrared spectrum of $[\text{Mn}(\text{PTMH})_2\text{Cl}_2]$ Schiff base complex

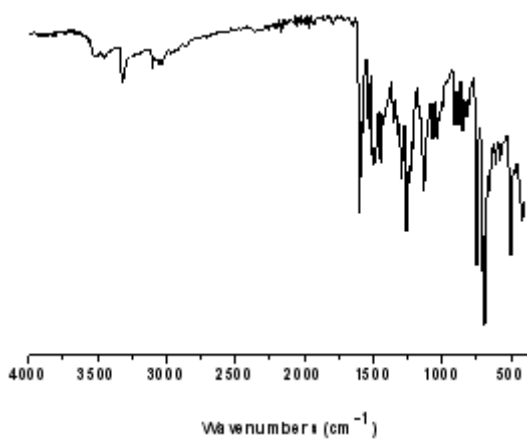


Fig. 2(c): Infrared spectrum of $[\text{Co}(\text{PTMH})_2(\text{NO}_3)_2]$ Schiff base complex

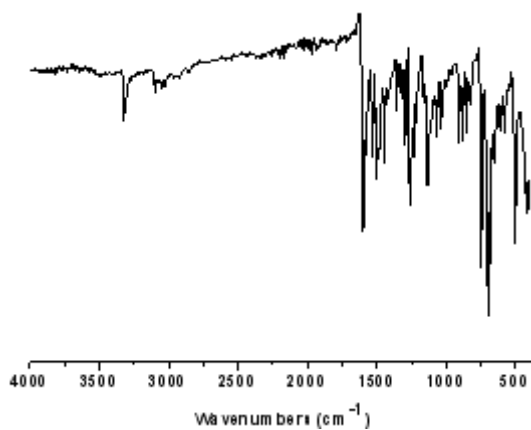


Fig. 2(d): Infrared spectrum of $[\text{Cu}(\text{PTMH})_2\text{Cl}_2]$ Schiff base complex

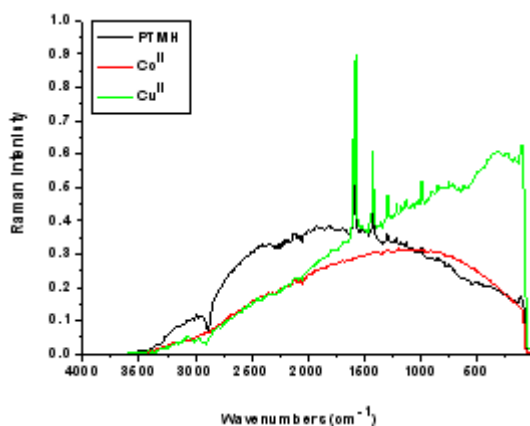


Fig. 3: Raman spectra of PTMH, $[\text{Co}(\text{PTMH})_2(\text{NO}_3)_2]$ and $[\text{Cu}(\text{PTMH})_2\text{Cl}_2]$ Schiff base complexes

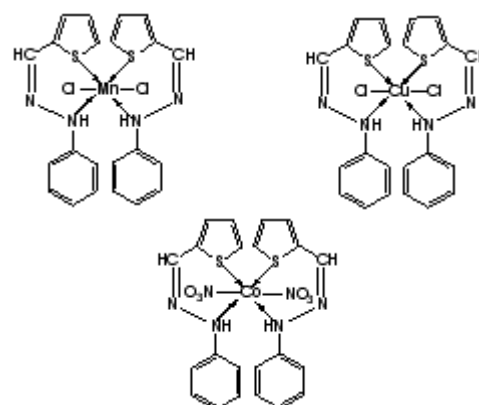


Fig. 4: Proposed structures of $[\text{Mn}(\text{PTMH})_2\text{Cl}_2]$, $[\text{Co}(\text{PTMH})_2(\text{NO}_3)_2]$ and $[\text{Cu}(\text{PTMH})_2\text{Cl}_2]$ Schiff base complex

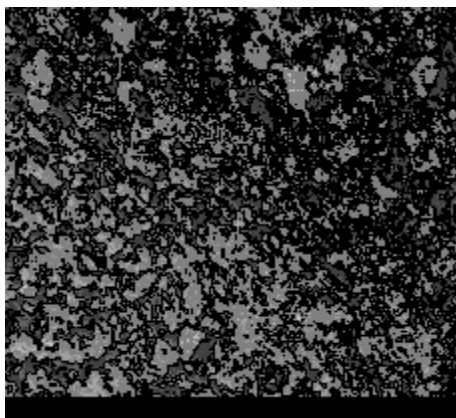


Fig. 5(a): Scanning Electron Microscope image of synthesized MnO nanoparticles for $[\text{Mn}(\text{PTMH})_2\text{Cl}_2]$ Schiff base complex at 3 h in 600°C

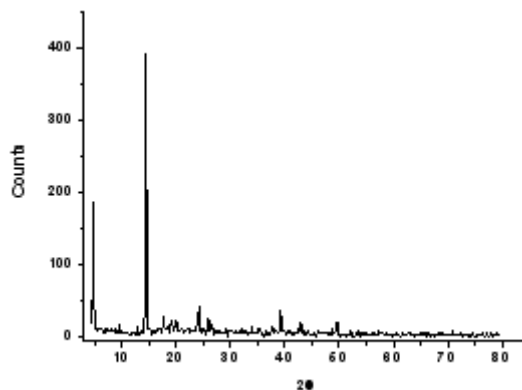


Fig. 6(a): XRD patterns of MnO nanoparticles

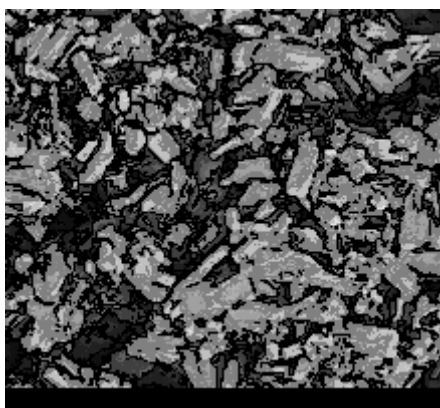


Fig. 5(b): Scanning Electron Microscope image of synthesized CoO nanoparticles for $[\text{Co}(\text{PTMH})_2(\text{NO}_3)_2]$ Schiff base complex at 3 h in 600°C

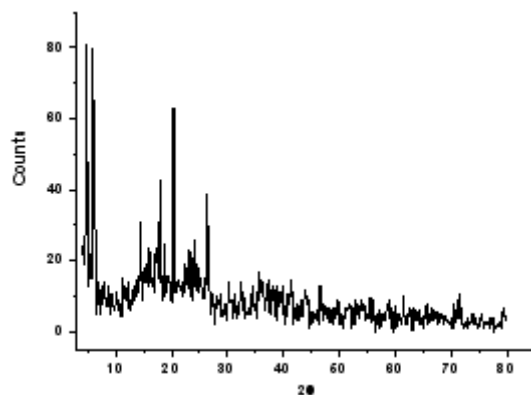


Fig. 6(b): XRD patterns of CoO nanoparticles

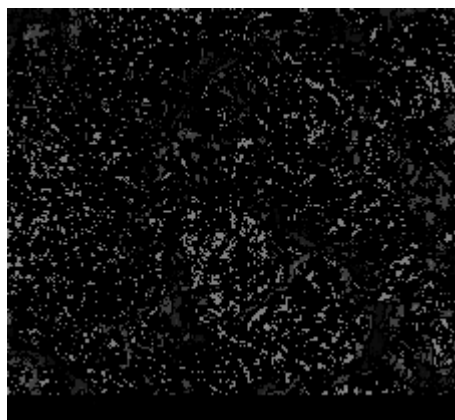


Fig. 5(c): Scanning Electron Microscope image of synthesized MnO nanoparticles for $[\text{Cu}(\text{PTMH})_2\text{Cl}_2]$ Schiff base complex at 3 h in 600°C

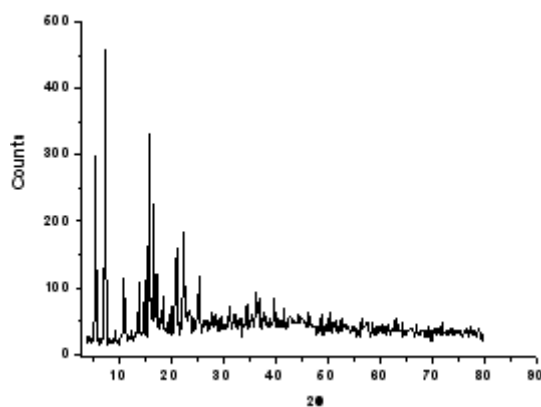


Fig. 6(c): XRD patterns of CuO nanoparticles

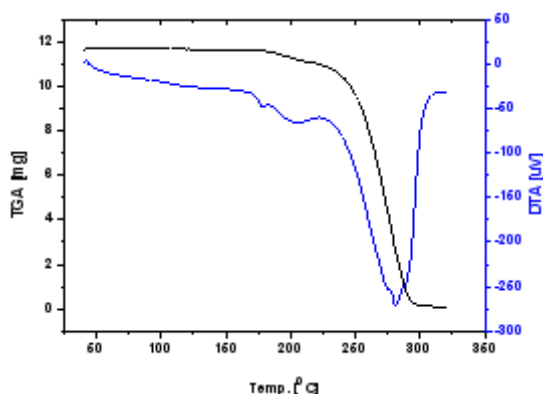


Fig. 7(a): TGA/DTA curves of PTMH Schiff base ligand

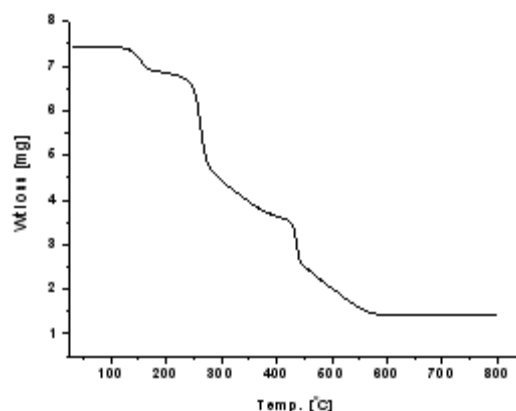


Fig. 7(b): TGA curve of $[Mn(PTMH)_2Cl_2]$ Schiff base complex

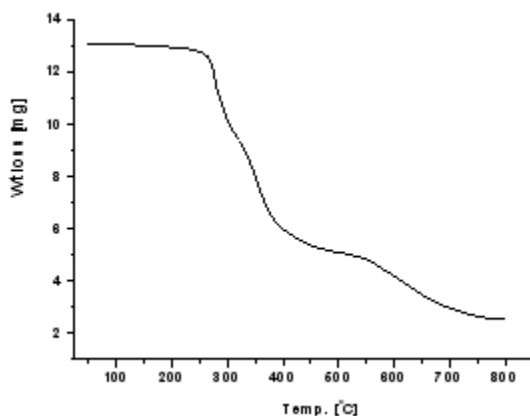


Fig. 7(c): TGA curve of $[Co(PTMH)_2(NO_3)_2]$ Schiff base complex

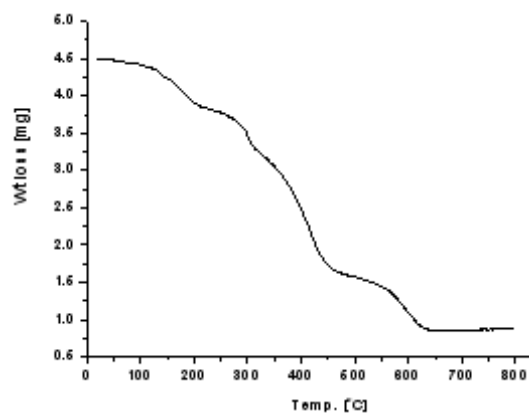


Fig. 7(d): TGA curve of $[Cu(PTMH)_2Cl_2]$ Schiff base complex

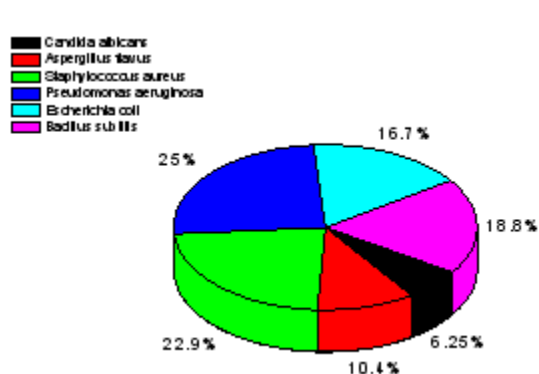


Fig. 8(a): Antimicrobial activity of PTMH

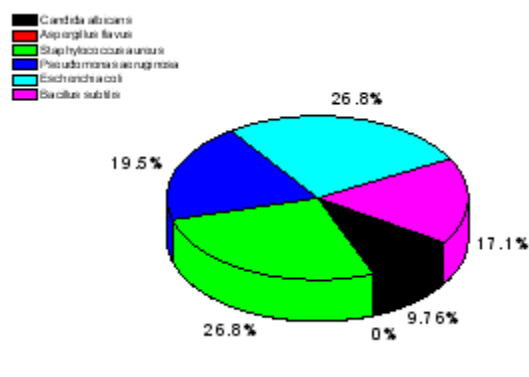


Fig. 8b: Antimicrobial activity of $[Mn(PTMH)_2Cl_2]$ Schiff base complex

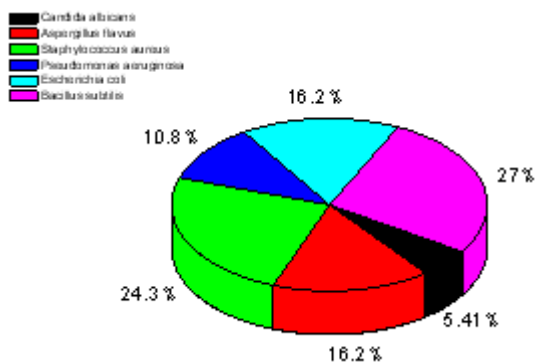


Fig. 8c: Antimicrobial activity of $[\text{Co}(\text{PTMH})_2(\text{NO}_3)_2]$ Schiff base complex

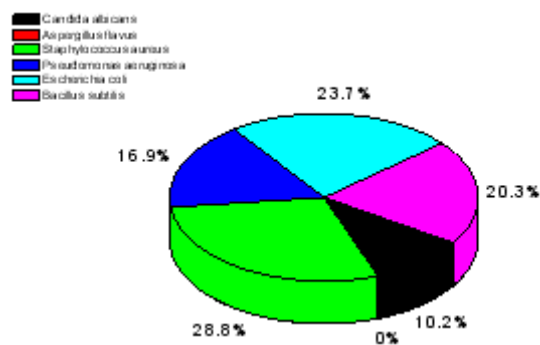


Fig. 8d: Antimicrobial activity of $[\text{Cu}(\text{PTMH})_2\text{Cl}_2]$ Schiff base complex

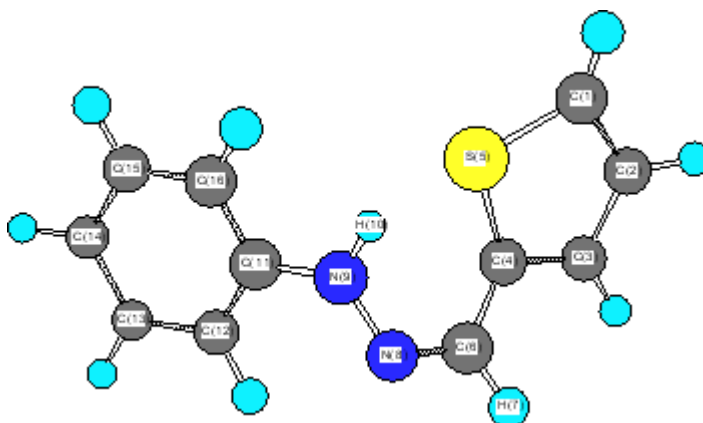


Fig. 9(a): Molecular modeling of PTMH Schiff base ligand

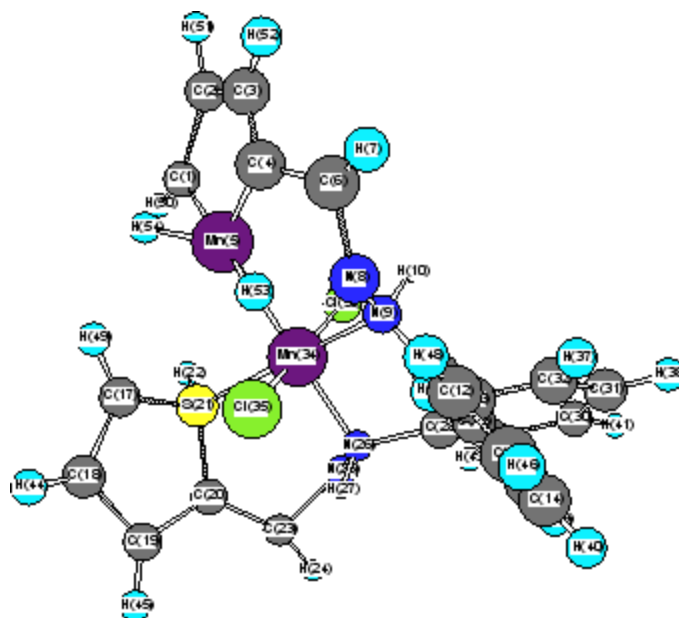


Fig. 9(b): Molecular modeling of $[\text{Mn}(\text{PTMH})_2(\text{Cl})_2]$ Schiff base ligand

that the size of the MnO, CoO and CuO nanoparticles was about 100-150 nm.

The thermal behavior of N-Phenyl-N'-thiophen-2-ylmethylene-hydrazine Schiff base ligand (Fig. 7a) shows two endothermic peaks at $DTA_{max} = 203$ and 280 °C with weight loss 100% in static air till steady state at 300 °C. The data respected to the thermal decomposition of the synthetic manganese(II), cobalt(II) and copper(II) PTMH Schiff base complexes were discussed. The TGA curve corresponding to the $[Mn(PTMH)_2Cl_2]$ Schiff base complex heated in the 30 °C till constant at 600 °C, temperature range are exhibited in Fig. 7b. The thermal decomposition of Mn(II) complex has three strong-to-medium peaks recorded in DTG curve at 163 , 293 and 443 °C. These steps are endothermic and assigned to the loss of 2PTMH and Cl_2 gas with weight loss 80.76%. Thermal analysis for $[Co(PTMH)_2(NO_3)_2]$ Schiff base complex has confirmed the thermal stability and the number of degradation steps upon to the DTG maximum peaks. According to TG curve (Fig. 7c) profiles have comprises at least two decomposition steps at 384 and 660 °C, both of them are endothermic process assigned to the completely decomposition of 2PTMH and $2NO_3$ with weight loss 80.73%. The TGA curve corresponding to the $[Cu(PTMH)_2Cl_2]$ Schiff base complex heated in the 30 °C till constant at 800 °C, temperature range are exhibited in Fig. 7d. The thermal decomposition of Mn(II) complex has three medium-to-weak peaks recorded in DTG curve at 197 , 367 and 450 °C. These steps are endothermic and assigned to the loss of 2PTMH and Cl_2 gas with weight loss 80.83%. It is an interesting result, that the calcination temperatures to get metal oxide in pure form take place at low temperature upon using Schiff base as precursors. The antibacterial activity of the Schiff base and its Mn(II), Co(II) and Cu(II) complexes against gram-positive (*Bacillus subtilis* and *Staphylococcus aureus*) and gram-negative (*Escherichia coli* and *Pseudomonas aeruginosa*) and two strains of fungus (*Aspergillus flavus* and *Candida albicans*) were studied. The antibacterial and antifungal results are shown in Table 3 and Fig. 8a-d.

All the Schiff base complexes individually exhibited varying degrees of inhibitory effect on the growth of the tested bacterial species. Table 3 shows that the activity of the Schiff base complexes became more pronounced when coordinated with the metal ions. The biological activity of the complexes follow the order: $Cu(II) > Mn(II) > Co(II)$.

Molecular modeling had been successfully used to detect three dimensional arrangements of atoms in free N-Phenyl-N'-thiophen-2-ylmethylene-hydrazine (PTMH) Schiff base ligand and its manganese(II), cobalt(II) and copper(II) complexes. The bond lengths and bond angles values of the chelation complex were summarized and refereed in Table 4 and Figs. 9a-c. These calculation for $[Mn(PTMH)_2Cl_2]$, $[Co(PTMH)_2(NO_3)_2]$, $[Cu(PTMH)_2Cl_2]$ complex was obtained by using the commercial available molecular modeling software Chem Office Ultra-7. These statistical data have a good agreement with Fig. 4 confirmed the place of coordination towards metal(II) ions.

CONCLUSIONS

In this paper we reported the preparation, isolation, and characterization of a new bidentate Schiff base derived from 2-thiophenecarboxaldehyde and phenylhydrazine, and its complexes with Mn(II), Co(II) and Cu(II) and using these complexes as precursors in the preparation of oxides in nano-sized particles. The synthesized metal complexes, in comparison to the un-complexed Schiff base ligand, were screened for their antibacterial and antifungal activities. The activity of the Schiff base complexes became more pronounced when coordinated with the metal ions.

ACKNOWLEDGEMENTS

This work was supported by grants from Vice President for Graduate Study and Research, Dammam University, Saudi Arabia under project Grants No. 2012051.

REFERENCES

1. A.H. Osman, *Transition Met. Chem.* **31**: 35 (2006).
2. D. Chen and A.E. Martel, *Inorg. Chem.* **26**: 1026 (1987).
3. J. Costamagna, J. Vargas, R. Latorre, A. Alvarado and G. Mena, *Coord. Chem Rev.* **119**: 67 (1992).
4. M. Cindrić, N. Strukan, V. Vrdoljak, T. Kajfež and B. Kamenar, *Croatica Chim. Acta* **76**: 157 (2003).
5. D.E. Chavez and E.N. Jacobsen, *Org. Lett.*, **5**: 2563 (2003).
6. X.Gao and D.G. Hall, *J. Am. Chem. Soc.*, **125**: 9038 (2003).
7. S.S. Djebbar, B.O. Benali and J.P. Deloume, *Transition Met. Chem.* **23**: 443 (1998).
8. Y.J. Hamada, *IEEE Trans. Electron Devices* **44**: 1208 (1997).
9. R. Ramesh and M. Sivagamasundari, *Synth. React. Inorg. Met.-Org. Chem.* **33**: 3 (1998).
10. A.D. Naik, S.M. Annigeri, U.B. Gangadharmath, V.K. Revankar and V.B. Mahale, *J. Mol. Struct.* **616**: 119 (2002).
11. C. Dowling and G. Perkin, *Polyhedron* **15**: 2463 (1996).
12. J.R.J. Sorenson and H. Siegel, In: Metal ions in biological system. New York – Basel, Dekker M., Inc. 78 (1982)
13. P. Gong, B. Hu, D. Stewart, M. Ellerbe, Y.G. Figueroa, V. Blanki, B.S. Beckman, J. Alam, *J. Biol. Chem.* **276**: 27018 (2001).
14. R. Moscovici, J.P. Ferraz, E.A. Neves, J.O. Tognoli, M.I. El Seoud, L. do Amaral, *J. Org. Chem.*, **41**(26): 4093 (1976).
15. C. Spinu, M. Pleniceanu, C. Tigae, *Turk. J. Chem.*, **32**: 487 (2008).
16. A.W. Bauer, W.M. Kirby, C. Sherris, M. Turck, *Amer. J. Clinical Pathology*, **45**: 493 (1966).
17. M.A. Pfaller, L. Burmeister, M.A. Bartlett, M.G. Rinaldi, *J. Clin. Microbiol.* **26**: 1437 (1988).
18. National Committee for Clinical Laboratory Standards, Performance Vol. antimicrobial susceptibility of Flavobacteria (1997).
19. National Committee for Clinical Laboratory Standards. Methods for dilution antimicrobial susceptibility tests for bacteria that grow aerobically. Approved standard M7-A3. National Committee for Clinical Laboratory Standards, Villanova, Pa (1993).
20. National Committee for Clinical Laboratory Standards. Reference Method for Broth Dilution Antifungal Susceptibility Testing of Conidium-Forming Filamentous Fungi: Proposed Standard M38-A. NCCLS, Wayne, PA, USA (2002).
21. National Committee for Clinical Laboratory Standards., Methods for Antifungal Disk Diffusion Susceptibility Testing of Yeast: Proposed Guideline M44-P. NCCLS, Wayne, PA, USA (2003).
22. L.D. Liebowitz, H.R. Ashbee, E.G.V. Evans, Y. Chong, N. Mallatova, M. Zaidi, D. Gibbs, and Global Antifungal Surveillance Group. *Diagn. Microbiol. Infect. Dis.* **4**: 27 (2001).
23. M.J. Matar, L. Ostrosky-Zeichner, V.L. Paetznick, J.R. Rodriguez, E. Chen, J.H. Rex, *Antimicrob. Agents Chemother.*, **47**: 1647 (2003).
24. M.H. Salunke, Z.A. Filmwala and A.D. Kamble, *Orient. J. Chem.*, **27**(3): 1243-1248 (2011).
25. S.E.J. Bell, N.M.S. Sirimuthu, *Chem. Soc. Rev.* **37**: 1012 (2008).
26. M.R. Kagan, R.L. McCreery, *Anal. Chem.* **66**: 4159 (1994).
27. A.B.P. Lever, *Coord. Chem. Rev.*, **3**: 119 (1968).
28. D.D. Bui, J. Hu, P. Stroeven, *Cem. Concr. Compos.* **27**: 357 (2005).